

# PHYSICAL PARAMETERS OF ERUPTING LUMINOUS BLUE VARIABLES: NGC 2363-V1 CAUGHT IN THE ACT<sup>1</sup>

Laurent Drissen<sup>2</sup>, Paul A. Crowther<sup>3</sup>, Linda J. Smith<sup>3</sup>, Carmelle Robert<sup>2</sup>, Jean-René Roy<sup>2</sup> and D. John Hillier<sup>4</sup>

(2) Département de Physique, Université Laval and Observatoire du mont Mégantic  
Qubec QC G1K 7P4, Canada

(3)Department of Physics and Astronomy, University College London  
Gower Street, London, WC1E 6BT, UK

(4)Department of Physics and Astronomy, University of Pittsburgh  
Pittsburgh, PA 15260

## ABSTRACT

A quantitative study of the Luminous Blue Variable NGC 2363-V1 in the Magellanic galaxy NGC 2366 ( $D = 3.44$  Mpc) is presented, based on ultraviolet and optical *Hubble Space Telescope* STIS spectroscopy. Contemporary WFPC2 and William Herschel Telescope imaging reveals a modest V-band brightness increase of  $\sim 0.2$  mag per year between 1996 January–1997 November, reaching  $V=17.4$  mag, corresponding to  $M_V=-10.4$  mag. Subsequently, V1 underwent a similar decrease in V-band brightness, together with a UV brightening of 0.35 mag from 1997 November to 1999 November.

The optical spectrum of V1 is dominated by H emission lines, with Fe II, He I and Na I also detected. In the ultraviolet, a forest of Fe absorption features and numerous absorption lines typical of mid-B supergiants (such as Si II, Si III, Si IV, C III, C IV) are observed. From a spectral analysis with the non-LTE, line-blanketed code of Hillier & Miller (1998), we derive stellar parameters of  $T_*=11\text{kK}$ ,  $R_*=420R_\odot$ ,  $\log(L/L_\odot)=6.35$  during 1997 November, and  $T_*=13\text{kK}$ ,  $R_*=315R_\odot$ ,  $\log(L/L_\odot)=6.4$  for 1999 July. The wind properties of V1 are also exceptional, with  $\dot{M} \simeq 4.4 \times 10^{-4} M_\odot \text{ yr}^{-1}$  and  $v_\infty \simeq 300 \text{ km s}^{-1}$ , allowing for a clumped wind (filling factor = 0.3), and assuming H/He~4 by number.

The presence of Fe lines in the UV and optical spectrum of V1 permits an estimate of the heavy elemental abundance of NGC 2363 from our spectral synthesis. Although some deficiencies remain, allowance for charge exchange reactions in our calculations supports a SMC-like metallicity, that has previously been determined for NGC 2363 from nebular oxygen diagnostics.

Considering a variety of possible progenitor stars, V1 has definitely undergone a giant eruption, with a substantial increase in stellar luminosity, radius, and almost certainly mass-loss rate, such that its stellar radius increased at an average rate of  $\sim 4 \text{ km s}^{-1}$  during 1992 October – 1995 February. The stellar properties of V1 are compared to other LBVs, including  $\eta$  Car and HD 5980 during its brief eruption in 1994 September, the latter newly analyzed here. The mass-loss rate of the HD 5980 eruptor compares closely with V1, but its bolometric luminosity was a factor  $\sim 6$  times larger.

*Subject headings:* stars: early-type – stars:mass-loss – stars: variables: other – stars: individual: NGC 2363-V1

---

<sup>1</sup>Based on observations with the NASA/ESA *Hubble Space Telescope*, obtained at the Space Telescope Science Institute, which is operated by AURA, Inc., under NASA contract NAS5-26555.

## 1. INTRODUCTION

Luminous Blue variables (LBVs) are evolved massive stars which display photometric and spectroscopic variability with different timescales and amplitudes. Although LBVs show micro-variations ( $\Delta\text{mag} \simeq 0.1$ - $0.3$  mag;  $\Delta t \sim \text{days-months}$ ) like other supergiants, it is their moderate “excursions” ( $\Delta\text{mag} \simeq 1$ - $2$  mag at constant  $M_{bol}$ ;  $\Delta t \sim \text{years}$ ) and giant eruptions ( $\Delta\text{mag} > 3$  mag with an increase in  $M_{bol}$ ;  $\Delta t \sim \text{years-decades}$ ) that define them as a class. They are found in the upper left section of the H-R diagram, having  $M_{bol} \leq -9$  and  $\log(T_{eff}) \geq 4.1$  (except during an eruption when their surface temperature often drops to  $\log(T_{eff}) \simeq 3.85$ ). LBVs are often, but not always, surrounded by a small (1-3 pc) nebula resulting from a giant eruption. We refer the reader to Humphreys & Davidson (1994) and Nota & Lamers (1997) for comprehensive, recent reviews on the subject. Although it is now widely accepted that the LBV phenomenon represents a normal yet unstable evolutionary phase in the life of the most massive stars, the exact mechanism leading to the major eruptions is still unknown. This lack of understanding is due in part to the problems involved in the theoretical modeling of the eruption phenomenon (Stothers 1999b), but also to the rarity of such events which has until recently prevented us from determining the physical parameters of an LBV *during* an eruption.

In 1996, we reported the discovery of a bright variable star in the giant extragalactic H II region NGC 2363 (Drissen, Roy & Robert 1996, 1997, hereafter DRR97). This star, known as NGC 2363-V1 (hereafter V1), was first noticed in HST/WFPC2 images. An archival search for ground-based images allowed us to determine that this star was below the detection limit in 1991 and 1992 ( $V \geq 21.5$ ), but became visible in late 1993. In early 1995, it became the brightest star in its galaxy, with  $V = 18.0$  mag. The photometric behavior, absolute magnitude and the presence in its spectrum of a strong H $\alpha$  emission line suggested that V1 is an LBV currently experiencing a major eruption event.

The host of the current LBV event is the giant H II region NGC 2363, located at the end of the bar in the Magellanic galaxy NGC 2366 ( $D = 3.44$  Mpc; Tolstoy *et al.* 1995). The metallicity of NGC 2363 has generally been determined to be close to that of the SMC (Gonzalez-Delgado *et al.* 1994), but Luridiana, Peimbert & Leitherer (1999) suggest that the metallicity of this region has been underestimated, and that a value of  $Z = 0.25Z_{\odot}$  would give a better fit to the observed line ratios. A detailed study of the stellar content of NGC 2363 (Drissen *et al.* 2000) reveals that two clusters of different ages are responsible for the ionization of the nebula. The main contributor is a very young (1 Myr or less), dense cluster of massive stars still embedded in their natal molecular cloud. V1 is a member of the second cluster, which is between 3 and 5 Myr old and contains 3 Wolf-Rayet stars.

Given the importance of this star in our understanding of the LBV phenomenon, we proposed a spectroscopic and photometric follow-up of V1 with the *Hubble Space Telescope*. This project was granted the long-term status for cycles 7 to 9 (GO- 7391, 8403 and 8781). We present in this paper an analysis of HST/STIS spectrograms obtained in 1997 November and 1999 July, covering the wavelength range 1180 Å to 1 $\mu\text{m}$ , supplemented by ground-based and HST photometry. We present our new observations in § 2 and produce a quantitative analysis with the non-LTE line blanketed code of Hillier & Miller (1998) in § 3. A plethora of Fe II lines in the UV and optical spectrum of V1 permits an estimate of the heavy metal content for NGC 2363. Our results are discussed in § 4, with conclusions reached in § 5.

## 2. OBSERVATIONS

DRR97 published a light curve of NGC 2363-V1 between 1991–1996 revealing a dramatic increase of  $\geq 3.5$  mag in brightness, although no color information was available. In this section, we present recent HST/WFPC2 and ground-based imaging, plus HST/STIS spectroscopy.

### 2.1. Photometry

UBVRI images of V1 were obtained on the night of 1998 January 14/15 with the 4.2 m William Herschel Telescope (WHT) on La Palma, Canary Islands. The Cassegrain auxiliary port was used with a Tektronix  $1024 \times 1024$  CCD ( $0.^{\prime\prime}11/\text{pixel}$ ). The exposure times were 300 s at BVRI and 600 s at  $U$ . The seeing was measured to be  $0.9\text{--}1.^{\prime\prime}0$ , sufficient to resolve V1 from the nearby H II region. Landolt (1992) standard star fields (98 624, 98 626 and 98 634) were also observed to provide the zero point calibration for the V1 images.

Accurate magnitudes for V1 are impossible to obtain using conventional aperture photometry because of severe contamination from the nearby H II region. The following approach was therefore adopted. Magnitudes were measured using a 35 pixel aperture with DAOPHOT (Stetson 1987) for several isolated stars in the same frames as V1. The same stars and V1 were then measured using a much smaller aperture of 3.5 pixels, and sky inner and outer radii of 4 and 7 pixels. These values were chosen to minimize the H II region contamination. The UBVRI magnitudes of V1 were then determined by assuming that the same fraction of light has been excluded from the smaller apertures for all the measured stars.

We also obtained WFPC2 photometry with the F170W, F336W, F547M and F1042M filters on 1998 March and December, 1999 November and 2000 February. The images were processed with the standard pipeline and aperture photometry of V1 was performed with DAOPHOT. The prescriptions given by Whitmore (1995) and Holtzman *et al.* (1995) were then followed to transform the instrumental magnitudes into the Johnson system.

Finally, near-infrared imagery of NGC 2363 were obtained in 1997 January by D. Devost and R. Doyon with the Monica Camera attached to the Canada-France-Hawaii telescope, which is described in more details in Drissen *et al.* (2000). From these observations, we get  $J=17.6$  ( $\pm 0.1$ ),  $H = 17.2$  ( $\pm 0.1$ ) and  $K = 16.9$  ( $\pm 0.2$ ). These values are slightly fainter than the predicted magnitudes based on the models described in the next sections ( $J = 17.1$ ,  $H = 16.9$  and  $K = 16.7$ ), indicating that cold dust has not yet formed in the stellar outflow.

The results of all photometric measurements are given in Table 1. The agreement between the ground-based and HST March data (taken 6 weeks apart) is very good in the V band, but the difference in  $U$  (0.6 mag) is significant. An updated light curve with the new data (in the V band) is shown in Figure 1. After the original outburst in 1993–1995, the brightness increase has been much more modest, though constant during 1996–1997, with a rate of  $\sim 0.2$  mag per year, as if the star had reached a state of quasi-equilibrium. The 1998–2000 photometric observations suggest a small, but comparable, faintening in the V band. The WFPC2 data also indicate that V1 brightened by  $\sim 0.3$  mag at 170 nm between 1998 March and 2000 February; during the same period, it faded by about the same amount at  $1 \mu\text{m}$ .

## 2.2. Spectroscopy

We obtained HST/STIS spectra of NGC 2363-V1 in 1997 November and 1999 July, using the MAMA detectors short ward of 3000Å and the CCDs at longer wavelengths. Because of the sensitivity of the MAMA detectors to high radiation levels in the South Atlantic Anomaly, the 1997 optical and UV spectrograms of V1 had to be acquired on separate occasions three weeks apart (November 2 and 21). Given the relative photometric stability of V1 between 1997 November and 1998 December, we do not expect that the spectroscopic appearance of the star has significantly changed during this short interval. In 1999, the optical and UV spectra were obtained 2 days apart. The following gratings were used: G140L (160 minutes) and G230L (90 minutes) with the MAMA detector; G430L (50 minute exposure), G750L (35 minutes) and G750M ( $\text{H}\alpha$ , medium resolution; 50 minutes) with the CCD detector. The 0.2 arcsecond-wide slit was used in all cases, which corresponds to a linear scale of 3 pc at the distance of NGC 2366.

Because the data originally processed with the standard HST pipeline showed unexplained anomalies, we have retrieved our data from the Canadian Astronomical Data Center (CADC). The CADC archives uses the best available calibration files to re-calibrate the data. Moreover, because V1 is located in the NGC 2363 nebula, extra care has been taken in subtracting the adjacent nebular spectrum from the spectrum of V1. Nebular contamination is small (V1 is in the middle of an expanding cavity) and relatively easy to subtract in the high (spatial) resolution STIS data compared with the highly contaminated ground-based spectra, but the standard pipeline calibration did not do a good job in this respect. Standard IRAF procedures were used. Despite the use of contemporary flatfield calibrations, the far red portion of the spectra is contaminated by fringing. By convolving our observed spectrophotometry with suitable synthetic filters, we obtained wide-band Johnson photometry (see Table 1) that is in excellent agreement with WFPC2 imaging.

The low-resolution flux calibrated HST datasets are presented in Figure 2. Balmer emission lines are the most prominent spectral features in the visible; weaker lines at  $\text{He I } \lambda 4471, 5876, 6678$ ,  $\text{Na I } \lambda 5890$  plus numerous  $\text{Fe II}$  transitions are also observed. The apparently noisy near-UV depression results from many Fe-transitions, rather than high interstellar reddening.

Since individual features are generally unresolved with the low resolution gratings, we have also obtained higher resolution  $\text{H}\alpha$  STIS observation with the G750M grating for each epoch. These are presented in Figure 3 and reveal a very strong  $\text{H}\alpha$  P Cygni profile betraying the extent of V1's envelope and its high mass-loss rate. The observed  $\text{H}\alpha$  flux is  $5.6 \times 10^{-14}$  and  $6.3 \times 10^{-14}$   $\text{ergs}^{-1} \text{cm}^{-2}$  for 1997 November and 1999 July, respectively. Correcting for interstellar reddening (see below) and the distance to NGC 2363, the intrinsic  $\text{H}\alpha$  luminosity of V1 is  $2.4\text{--}2.7 \times 10^4 L_\odot$ .

While the general appearance of the spectrum is similar at both epochs, a few changes are worth noting:

(1) The UV continuum flux (1200 - 2800 Å) is stronger in 1999. However, the line fluxes in this wavelength range has not changed significantly.

(2) The strength and profile of the Balmer lines has changed (see Table 2). The flux of the  $\text{H}\alpha$  line in the July 99 dataset is  $\sim 20\%$  stronger and its blue absorption component extends to higher velocities (Figure 3). On the other hand, the equivalent widths of the other Balmer lines have slightly decreased and the absorption components of their P Cygni profile are less deep in 1999.

(3) The  $\text{Fe II}$  lines at 4925 and 5016 Å which were strong in the 1997 data became much weaker in 1999.

### 2.3. Morphology of the UV spectrum

The resolution of the STIS data ( $\sim 300$  km s $^{-1}$ ) does not allow us to easily, and unequivocally, distinguish between the interstellar and purely stellar contribution components to the resonance lines on the basis of their width alone. But a direct comparison of the line strengths between the spectrum of V1 and those of knots NGC 2363-A and B (obtained with HST/FOS; see Drissen *et al.* 2000 and Figure 4 here) should allow us to identify the lines which are intrinsic to the star's photosphere. We assume that since V1 and knot B are both located within the same expanding superbubble, the spectral contribution from their local ISM will be similar, although knot B is a cluster of OB stars and some ISM lines in its spectrum could be contaminated by a stellar contribution. On the other hand, the ISM local to knot A could be different, but contributions from OB stars are negligible. The contribution from Milky Way gas should be the same in all three objects. From Figure 4, which shows the rectified spectrum of V1 in 1999 in the range 1160 - 1700 Å along with that of knots A and B, and from Table 3, which lists the equivalent width of the most conspicuous UV lines in the three objects, we conclude that the UV lines of V1 have a strong photospheric contribution. As examples, one may compare the lines of Si II  $\lambda 1260$ , C II  $\lambda 1335$ , Si IV  $\lambda 1400$  and Si II  $\lambda 1527$ . None of these UV lines in V1 however show any evidence for an emission component, suggesting a rather low effective temperature.

The following lines are both strong in V1 and absent or very weak in the spectrum of knots A and B; they are thus likely to have a photospheric origin: C III  $\lambda 1175$ , Mg II  $\lambda 1240$ , Si II  $\lambda 1251,54,60$ , Si II  $\lambda 1265$ , Ti III+Si III between 1286 and 1303 Å, Si II  $\lambda 1309$ , and Si II  $\lambda 1533$ .

The C III  $\lambda 1175$  line typically shows a strong P Cygni profile in late-type O to early-type B supergiants and becomes mostly photospheric in mid B supergiants (Snow & Morton 1976). It is an obvious ( $W_\lambda = 2.4$  Å) absorption feature in V1, but appears much weaker than in late-type B supergiants such as  $\eta$  CMa (B5Ia) or  $\beta$  Ori A (B8Ia). Also, features seen in the spectrum of V1 between 1295 and 1303 Å, are often associated to Si III in B stars (Massa 1989). Therefore in Figure 4, we have plotted along with V1 the rectified spectrum of an average Galactic B5.5I star (based on high resolution IUE spectra of 4 B6I and B5I stars from the library of Robert 1999). The resolution of this B5.5I spectrum was degraded to mimic the STIS data. Similarities with V1 are striking. In the following discussion we compare the spectral feature of V1 with those of B stars.

The strength of the Si II  $\lambda 1265$  line is a strong (inverse) function of the effective temperature in OB stars, but insensitive to the luminosity class (Massa 1989; Prinja 1990), increasing from 100 mÅ at  $T_{eff} = 25000$ K to 1600 mÅ at  $T_{eff} = 13000$ K. Si II  $\lambda 1265$  is not seen in stars hotter than B0. The large value of  $W_\lambda$  (Si II  $\lambda 1265$ ) = 1800 mÅ in the 1999 spectrum of V1 sets a relatively stringent upper limit of  $T_{eff} \leq 13000$ K, albeit based on a Galactic supergiant calibration.

The strong line at  $\sim 1303$  Å is a blend of stellar and interstellar lines. The interstellar component (mostly O I  $\lambda 1302$  and Si II  $\lambda 1304$ ) dominates in knots A and B (total  $W_\lambda = 2.2$  Å in both cases), but the blend is stronger in V1 ( $W_\lambda = 4$  Å), indicating a strong photospheric contribution from Si III  $\lambda 1301,03$  and Si II  $\lambda 1304$  typical of late to mid-B stars.

The Si II  $\lambda 1309$  line behaves like Si II  $\lambda 1265$  as a function of OB spectral types. The Si II  $\lambda 1533$  is more difficult to study in hot OB stars as the broad wind profiles developing in C IV  $\lambda 1550$  engulfs it and as it is blended with Fe IV (Nemry *et al.* 1991) in hotter stars. Nevertheless there are indications that Si II  $\lambda 1533$  is also a good B star signature.

Spectral features around 1317, 1345, and 1455 Å, which are associated with Ni II, P III, and Ti III, are typical of B supergiants; they are not seen in giants and dwarfs B (except maybe in the earliest types B0-1).

The strength of the doublet Si IV  $\lambda 1394, 1402$  is strongly temperature and luminosity dependent (Walborn *et al.* 1995). It is absent from all late B luminosity classes, appears in absorption in mid-early types, and in the case of the early B supergiants shows a strong P Cygni wind profile. An absorption doublet of C IV  $\lambda 1549, 51$  is only seen in hot B0-2 dwarfs and giants. A wind profile appears in the hottest giant B0. In the case of supergiants, the absorption is seen for mid B and quickly becomes a strong P Cygni profile in type B4 and hotter. We do not see Si IV and C IV wind profiles in V1 but rather absorption typical of B5-6 I stars.

Around 1600 Å we see many strong lines of Fe II and Fe III which resemble the features of B supergiants. These lines are much weaker in B giants and dwarfs.

We therefore conclude that the UV spectrum of V1 is similar to that of a B supergiant star of type 5-6.

### 3. SPECTROSCOPIC ANALYSIS

An important consideration for the interpretation of V1's spectral energy distribution is the determination of the extinction. Gonzalez-Delgado *et al.* (1994) derived  $E(B-V) \simeq 0.15$  mag from a ground-based integrated nebular spectrum of the whole H II region. Since the extinction is likely to be different in knot A, which dominates the global nebular spectrum, than in the middle of the expanding bubble where V1 and knot B lie, we have extracted the spectrum of the nebula from the pixels adjacent to V1 in the STIS long-slit spectroscopy. The nebular H $\alpha$ /H $\beta$  line strengths from this region reveal a low value of  $E(B-V) = 0.06$  using Case B recombination theory (Hummer & Storey 1995); this is in perfect agreement with Drissen *et al.* (2000) who recently estimated  $E(B-V) = 0.04$  (Galaxy) + 0.02 (NGC 2363) based on HST/FOC UV spectra of knot B in NGC 2363. Therefore, if an associated circumstellar nebula is present, it does not add measurably to the interstellar extinction, arguing against a dense,  $\eta$  Car-like nebula surrounding V1. We have thus reddened the theoretical continuum energy distributions by  $E(B-V) = 0.04$  using the Seaton (1979) Galactic extinction law, plus  $E(B-V) = 0.02$  using the Bouchet *et al.* (1985) SMC law. Assuming a distance of 3.44 Mpc to NGC 2366 implies  $M_V = -10.44$  mag during 1997 November, and  $-10.29$  in 1999 July.

For stars with extended atmospheres such as NGC 2363-V1, as evidenced from its P Cygni H $\alpha$  profile, the usual assumptions of plane parallel geometry and local thermodynamic equilibrium (LTE) are totally inadequate. In this section we introduce the atmospheric model that we shall use for V1 and discuss our analysis technique.

#### 3.1. Atmosphere code

We utilize the iterative, line blanketed technique of Hillier & Miller (1998) which solves the transfer equation in the co-moving frame subject to statistical and radiative equilibrium in an expanding, steady-state atmosphere. Populations and ionization structure are consistent with the radiation field. Line blanketing is treated via a global Doppler line width of  $V_{\text{Dop}} = 10 \text{ km s}^{-1}$ .

Despite the high quality dataset available, the spectroscopic analysis of NGC 2363-V1 has proved to be difficult, principally because its low excitation state means that Fe II is the dominant blanketing ion, which is extremely complex. In addition, as discussed by Hillier *et al.* (1998), mass-loss and hydrogen content are highly coupled. Since we are unable to tightly constrain the stellar temperature of V1, due to the absence of lines from adjacent ionization stages of the same element, we cannot derive a mass-loss rate without first fixing its He abundance. Consequently, we shall adopt an abundance of H/He=4 by number, which is typical

of LBVs (Crowther 1997), and subsequently investigate the effect of different He abundances on the mass-loss rate. Similarly, metal abundances were fixed at  $0.20Z_{\odot}$  as indicated by Gonzalez-Delgado et al. (1994) for NGC 2363, and varied once stellar parameters were derived.

A simplifying ‘super level’ approach is used for individual levels (Anderson 1989), particularly for iron-group elements. In this approach, several levels of similar energies and properties are treated as a single ‘super level’, with only the populations of the super level included in the solution of the rate equations. The population of an individual atomic level in the full model atom is determined by assuming that it has the same departure coefficient as the corresponding super level to which it belongs.

The present model include representative model atoms for H, He, N, Mg, Al, Na, Ca, Si and Fe, as indicated in Table 4, in which a total of 32,191 transitions are considered. Details of each ion are included, such that for hydrogen,  $n=1$  to 30 full levels are considered, which are grouped into 10 super levels. Our default atomic dataset for Fe II was taken from Nahar (1995), in which 827 atomic levels, were combined into 134 super levels, producing 21,907 transitions (22,924 weak transitions with  $\log gf < -4$  were omitted). Hillier et al. (2000) have recently analyzed the UV and optical spectrum of  $\eta$  Car based on the Nahar compilation and found improved comparisons with observation if Kurucz (1993) oscillator strengths were selected instead of those from Nahar, although negligible differences were obtained for V1.

In the outer wind of V1, and other LBVs, hydrogen becomes neutral, so it is necessary to allow for charge exchange reactions. Of particular relevance to LBVs is the charge exchange reaction:  $\text{Fe}^{2+} 3d^6(^5D) + \text{H} \leftrightarrow \text{Fe}^+ 3d^64s(^6D) + \text{H}^+$  (Neufeld & Dalgarno 1987) since the ratio of charge recombination to radiative recombination for  $\text{Fe}^{2+}$  is  $\sim 10^3$   $\text{H}/\text{H}^+$  (Hillier et al. 2000). This has a major influence on the ionization structure, and significantly enhances the Fe II line strengths. Also relevant to LBVs is the nitrogen reaction:  $\text{N}^{2+} + \text{He}^+ \leftrightarrow \text{N}^+ + \text{He}^{2+}$  (Herrero et al. 1995).

Finally, since it is well established that the dense winds of early-type stars are clumped (e.g. Lépine & Moffat 1999; Eversberg et al. 1998), we consider a relatively simple volume filling factor approach for V1 following Hillier & Miller (1998). Estimates of clumping factors in the optical line forming region for V1 are provided by simultaneously matching recombination emission line strengths (sensitive to the square of the density) and electron scattering wings (sensitive to density) as discussed by Hillier (1991).

### 3.2. Stellar parameters

Since we were unable to use lines from adjacent ionization stages of one particular element to derive stellar temperatures, we instead relied on the stellar continuum, de-reddened as described above. We have calculated a grid of models for V1 at each epoch in order to simultaneously match the stellar continuum distribution from which the stellar temperature and luminosity are derived, plus  $\text{H}\alpha$  which provides an excellent tracer of mass-loss in the winds of early-type stars (Puls et al. 1996). We have adopted a typical H/He content of LBVs for NGC 2363-V1, namely H/He=4 by number (see also below).

For the 1997 November dataset, we find optimum agreement for a model in which  $T_*=11\text{kK}$ ,  $\log(L/L_{\odot})=6.35$  and  $R(\tau_{\text{Ross}} = 10) = 420R_{\odot}$ , as shown in Figure 5 (upper panels). Since the atmosphere of NGC 2363-V1 is very extended,  $R(\tau_{\text{Ross}} = 2/3) = 590R_{\odot}$ , the formal ‘effective temperature’ is  $T_{\text{eff}}=9,200\text{K}$ . Similar properties for July 1999 are  $T_*=13\text{kK}$ ,  $\log(L/L_{\odot})=6.4$  and  $R(\tau_{\text{Ross}} = 10) = 315R_{\odot}$ , shown in Figure 5 (lower panels). Therefore, the spectroscopic differences between the two epochs represent variations in stellar radius (i.e. temperature) at fairly constant bolometric luminosity. This naturally explains the simultaneous UV

brightening and optical fading during this period.

While the agreement between the model and the observations is generally very good, we wish to highlight several important discrepancies revealed in this work. The sole helium line observed at high resolution with HST/STIS is He I  $\lambda 6678$ , which is observed in absorption for both epochs. It was hoped that we would have been able to determine H/He abundances from H $\alpha$  and He I, but the He I absorption is rather insensitive to the precise H/He abundance ratio, and more problematic, predicted absorption strengths are significantly weaker than observations.

Another important discrepancy is that the continuum fit to observations is imperfect, at both epochs; (a) Fe II blanketing is apparently underestimated between  $\lambda\lambda 1700$ -2300 using our determination of the iron content in V1 (see § 3.4); (b) the models clearly fail to reproduce the observed continuum distribution either side of the Balmer ‘jump’, by up to  $\sim 20\%$ . Hillier et al. (2000) experienced similar difficulties in their analysis of  $\eta$  Car (see § 3.5).

### 3.3. Mass-loss properties

In addition to deriving stellar parameters, we have simultaneously modeled the H $\alpha$  profile for each epoch by varying the mass-loss rate, and terminal velocity.

Using volume filling factors of  $\sim 30\%$ , which provide a reasonable match to the electron scattering wings of H $\alpha$ , we find an approximately constant  $\dot{M}=4.4\times 10^{-4}M_{\odot} \text{ yr}^{-1}$  for both epochs, such that the stronger H $\alpha$  emission in 1999 results from the increase in stellar temperature, rather than a change in mass-loss rate. Wind velocities are also very similar,  $v_{\infty}=325 \text{ km s}^{-1}$  and  $v_{\infty}=290 \text{ km s}^{-1}$  for 1997 November and 1999 July, respectively. Differences in H $\alpha$  absorption can be matched with different turbulent velocities,  $v_{\text{turb}}=10$  and  $40 \text{ km s}^{-1}$ . Comparisons between synthetic spectra and observations are shown in Figure 6.

An important caveat which should be kept in mind is that we have relied solely on H $\alpha$  as a mass-loss indicator, since all other Balmer lines are unresolved. Nevertheless, low dispersion HST/STIS observations reveal that the increase in strength of H $\alpha$  from 1997 to 1999 is not repeated for H $\beta$  and higher Balmer members (Table 2). Were we instead to rely on the H $\beta$  flux, our modeling would reveal a  $\sim 30\%$  decrease in mass-loss, rather than a constant rate, between the two epochs. Such differences in behavior amongst members of the Balmer series are not repeated amongst other LBV-type supergiants (e.g. HDE 316285: Hillier et al. 1998).

One further complication is that since we have used solely H $\alpha$  to constrain the mass-loss rate, this is also dependent on the atmospheric H/He composition. For a solar composition the clumped mass-loss rates would decrease to  $\sim 2.5 \times 10^{-4}M_{\odot} \text{ yr}^{-1}$ . Conversely, if V1 is more highly enriched (e.g. H/He=1 by number), we would need to increase the mass-loss rate estimate by a factor of  $\sim 2$  to  $10^{-3}M_{\odot} \text{ yr}^{-1}$ .

### 3.4. Metal Abundances

Unfortunately the low spectral resolution of our observations together with the narrow, weak emission from most metal ions means that the determination of elemental abundances is not possible. However, the presence of numerous optical Fe II transitions, together with a forest of metal lines in the near-UV permit an estimate of the iron abundance to be determined. Neglecting the effect of charge exchange would require

systematically higher abundances (at least by a factor of two) than we obtain here. Ideally, we would like to have used a similar star at known metallicity to check our modeling procedure against, but no such stars exist with parameters close enough to V1.

In Figure 7 we compare de-reddened ultraviolet observations of V1 from 1997 November with Fe II blanketed models at  $0.20Z_{\odot}$ ,  $0.5Z_{\odot}$  and  $1.0Z_{\odot}$  degraded to the resolution of the STIS spectroscopy. Each model provides a fair match to the observed continuum depression around  $2500\text{\AA}$  including the discontinuity at  $\lambda 2630$ . The  $0.20Z_{\odot}$  case compares very closely with observations in the  $\lambda\lambda 2500\text{--}2900$  region. The  $0.10Z_{\odot}$  model, not shown in this Figure, is marginally worse than the  $0.20Z_{\odot}$  case. Discrepancies remain for each case, especially at  $\lambda\lambda 1750\text{--}2300$ . We attribute such discrepancies to the shear complexity of the observed UV spectrum (Hillier et al. 2000 obtained similar problems for models of  $\eta$  Car). For example, in the case of the  $1.0Z_{\odot}$  model, 2878 lines are predicted to have equivalent widths of  $\geq 0.1\text{\AA}$  in the  $1200\text{--}3100\text{\AA}$  region. These are dominated by 2351 lines of Fe II and 416 lines of Fe III. In the light of model discrepancies between  $\lambda\lambda 1750\text{--}2300$ , a comparison with observations marginally favors the low metallicity cases, but is unable to provide a definitive abundance determination.

Figure 8 compares rectified observations in the  $3000\text{--}5500\text{\AA}$  region, with synthetic spectra covering the same range in metallicity. Aside from the Balmer series, the majority of features are again due to Fe II, the strengths of which are very sensitive to metal content. As for the UV, an SMC-like iron abundance for V1 is favored by the weakness of iron lines in the  $\lambda\lambda 3100\text{--}3500$ ,  $\lambda\lambda 4450\text{--}4600$  and  $\lambda\lambda 4900\text{--}5300$  regions. Unfortunately, prominent P Cygni Na I emission at  $\lambda 5890\text{--}6$  is not predicted sufficiently strong in any case, while comparisons in the far-red are prevented by significant CCD fringing.

Note, however, that caution is necessary. Although we include over 700 energy levels of Fe II in our calculations, this ion is extremely complex, with potentially imprecise atomic data. In addition, although Fe II is certainly the most prominent heavy element, ions of other less abundant elements will make significant contributions to the line blanketing at particular wavelengths (e.g. Ni II). Work is currently underway to include such elements in our calculations.

Further, we have based our iron abundance estimate on a comparison between models selected to match the 1997 November HST/STIS dataset. Were we instead to have used the 1999 July observation, we would have revealed a somewhat lower iron abundance, since the emission strength of optical Fe II lines (e.g.  $\lambda 5015$ ) is weaker at that epoch.

Nevertheless, we conclude that the heavy metal content of NGC 2363-V1 is  $\sim 0.2Z_{\odot}$ , in reasonable agreement with the previously derived nebular oxygen abundance of  $12+\log(\text{O/H})=7.9$ , a factor of six below the solar value. Recall that iron is produced by supernovae, whose progenitors have lifetimes of typically 1Gyr, while oxygen is created exclusively by short-lived, high mass stars. Our study represents the most distant star whose iron abundance has been derived, and compared with  $\alpha$ -elements.

### 3.5. Balmer jump – evidence for asymmetry?

The shape of the Balmer jump is notoriously difficult to reproduce in extreme OB supergiants. The case for V1 is no exception – from Figure 5 the model does not fit the continuum well on both sides of the Balmer jump. In fact, the model predicts a lower continuum level shortward of the Balmer edge while the observations clearly show an increasing flux below  $3700\text{\AA}$ . This is best illustrated for V1 in Figure 9, and includes HST/FOS spectra of two B stars in the LMC cluster Breysacher 73 (Walborn et al. 1999). The

spectral shape of V1 around the Balmer edge is quite similar to that of Brey 73-1C, an O9.5-B1pe star, classified as such because an emission component is clearly seen in the center of the Balmer absorption lines. The unusual flux increase from 3750 to 3650 Å which is seen in both stars, has been observed in a number of Be stars (Kaiser 1987) and has been interpreted as evidence for the existence of a disk-like extended envelope of low density around the stars. The mass-loss rate of V1 is much higher than that of Be stars and the two-component model may not be applicable in this case, but the peculiar shape of its continuum around the Balmer edge may indicate that its envelope is not spherically symmetric. Indeed, most nebulae around LBVs exhibit axisymmetric morphologies that could have been shaped by non-spherical mass loss (Nota *et al.* 1995). Spectropolarimetry of the H $\alpha$  line and its adjacent continuum could be used to measure the degree of asymmetry, if any, of V1’s envelope.

#### 4. DISCUSSION

Our results place tight constraints on the current stellar properties of NGC 2363-V1. Major LBV eruptions are thought to coincide with an increase in the bolometric luminosity of the star and probably also its mass-loss rate. We now consider whether V1 has undergone a genuine eruption, and subsequently compare its properties with other LBVs, notably HD 5980 during its brief eruption in 1994 (Barba & Niemela 1994).

##### 4.1. Is NGC 2363-V1 undergoing a genuine eruption?

Since the presence of NGC 2363-V1 was unknown prior to its recent brightening, no spectroscopic or photometric information is available to us in order to readily constrain its pre-outburst properties. Consequently, we consider three possibilities for its spectral type prior to 1993, namely an early O, late O, or early B supergiant.

For O3 and O8 supergiant cases, we adopt a temperature and bolometric correction scale from Vacca *et al.* (1996), together with mass-loss rate estimates following the wind momentum–luminosity relation of Puls *et al.* (1996) for low metallicity (mixture of LMC and SMC) stars. For the early B supergiant case, we consider the possibility that V1 was a dormant, hot LBV, equivalent to AG Car or R127 during their WN11 phase (e.g. Smith *et al.* 1994), whose wind properties are estimated from Crowther (1997). Properties derived in this way are presented in Table 5.

We first consider the possibility that V1 was a hot, dormant LBV immediately prior to 1993. In this case, the low bolometric correction would indicate that the luminosity of V1 would have been amongst the lowest of all known LBVs with  $\log(L/L_\odot) \leq 5.5$ , comparable with R110 (Stahl *et al.* 1990). In contrast, those LBVs which have been known to experience a very hot WN11 phase have luminosities in excess of  $\log(L/L_\odot) \geq 6$ . Nevertheless, for such a scenario, the increase in bolometric luminosity corresponds to a factor of approximately ten, with a mass-loss rate probably increasing by several hundred fold. We neglect the possibility that V1 was a cooler, P Cygni-type dormant LBV since its bolometric luminosity would then have been unrealistically low.

Alternatively, V1 may have advanced immediately from an O supergiant to an erupting LBV. The age of NGC 2363-B, from which V1 is thought to have originated is 3–5 Myr (Drissen *et al.* 2000), so an O8 supergiant progenitor represents a realistic possibility. In such a case, the increase in luminosity by V1 is

less severe (see Table 5), albeit a factor of four (or greater), while the increase in mass-loss rate is perhaps one thousand fold if the progenitor has wind characteristics comparable to Magellanic Cloud supergiants. The absence of cool dust around V1 favors an O supergiant progenitor rather than a dormant LBV.

The final possibility, is that V1 advanced directly from an O3 supergiant. These very young ( $\leq 2$ –2.5 Myr) stars have the highest bolometric corrections of any hot massive star, prior to the Wolf-Rayet phase. We consider this possibility highly unlikely, given their youth relative to NGC 2363-B. Nevertheless, for completeness, the change in stellar and wind properties would be the least severe, with potentially only a modest increase in luminosity, together with a factor of one hundred increase in mass-loss rate.

The rapid brightening of V1 also indicates a corresponding increase in the physical size of the star. Based upon a late O supergiant progenitor, the surface of V1 expanded from a radius of  $\sim 20$  to  $420R_{\odot}$  in a little over two years (1992 October to 1995 February), corresponding to an average rate of  $+4 \text{ km s}^{-1}$ ! This calculation assumes that the stellar temperature of V1 in early 1995 was comparable to that of 1997 November, which appears realistic considering the similarity in photometry (Table 1). Subsequently, between 1997 November and 1999 July, the radius of V1 decreased from  $420$  to  $315R_{\odot}$ , at an average rate of  $-1.4 \text{ km s}^{-1}$ . These changes support some form of pulsational or dynamical instability as the cause of the present eruption (e.g. Guzik et al. 1999; Stothers 1999a). Calculations in our group are underway to assess such possibilities.

In summary, it appears that V1 is a moderately massive star which underwent an dramatic increase in luminosity, radius and mass-loss rate between late 1992 and early 1995, with a probable late O-type supergiant or perhaps hot, dormant LBV progenitor. Estimating an initial mass for V1 is extremely difficult since this would rely on a comparison between the luminosity of the star prior to eruption with low metallicity evolutionary tracks (Meynet et al. 1994). Nevertheless, an age of 4–5 Myr suggests an initial  $40$ – $60M_{\odot}$  star, with a present luminosity of  $\log(L/L_{\odot}) = 5.8$ – $6.0$ , consistent with a late-type O supergiant precursor.

Consequently, we suggest that the initial and current mass of NGC 2363-V1 is no more extreme than many other LBVs, such as AG Car. In contrast, the initial mass of the Pistol star appears to be remarkably high ( $\geq 200M_{\odot}$ , according to Figer et al. 1998).

#### 4.2. Comparison between V1 and other LBVs

We have shown that V1 is currently undergoing a giant eruption, and that its stellar and wind properties are exceptional. What distinguishes V1 from ‘dormant’ LBVs, such as AG Car? How do these compare with HD 5980 which briefly underwent an eruption in a similar low metallicity environment during 1994?

The well known Galactic LBV AG Car is currently undergoing huge variations in temperature (from 8,000–25,000K) over timescales of decades. Its stellar properties have been studied by Leitherer et al. (1994) who found a fairly (homogeneous) mass-loss rate of  $\sim 10^{-5}M_{\odot}\text{yr}^{-1}$  at a constant luminosity of  $\log(L/L_{\odot})=6.1$ . Consequently, V1 is currently little more than a factor of two times more luminous than AG Car, which is surprisingly small. In contrast, the mass-loss rate of V1 is perhaps 50 times higher, and appears to be the principal defining characteristic (see below).

Are the properties of V1 during its present eruption typical of other massive stars? This question is particularly relevant to stellar evolution models of massive stars in which, brief episodes of very intensive mass-loss are predicted or assumed. To address this question, we have investigated the stellar properties of HD 5980 during its brief eruption (Barba & Niemela 1994) based on the optical spectroscopy obtained by

Heydari-Malayeri et al. (1997) during the visual maximum in 1994 September when  $V=8.6$  mag (Albert Jones, private communication). Based on an interstellar reddening of  $E(B-V)=0.07$  mag towards HD 5980 (Crowther 2000), together with an SMC distance modulus of 18.9 mag (Westerlund 1997), the absolute visual magnitude of the erupting star was  $M_V = -10.5$  mag (all other components play a negligible contribution to the continuum flux at this epoch). This is remarkably similar to the current absolute visual magnitude of V1. However, the spectral appearance of the HD 5980 eruptor was considerably different from V1 at visual maximum. Heydari-Malayeri et al. (1997) revealed a much hotter, WN11-type appearance (Fig. 10) so it was intrinsically much more luminous than V1.

We have analysed the optical spectrum of HD 5980 from Heydari-Malayeri et al. (1997), using the Hillier & Miller (1998) code. Based on the usual  $\text{He I } \lambda 4471$ ,  $\text{He II } \lambda 4686$  and  $\text{H}\beta$  diagnostics, our derived parameters are listed in Table 4, revealing that the luminosity of the HD 5980 eruptor exceeded both V1 and  $\eta$  Car by a factor 3–6, respectively. Indeed the only other LBV whose luminosity may compare favourably with HD 5980 is the Pistol star (Figer et al. 1998), although analysis of it is severely hampered by the high reddening plus lack of definitive temperature constraints. A comparison between our new results for HD 5980 with those of Koenigsberger et al. (1998) based on observations from 1994 December (when it had visually faded by 1.6 mag) suggests that its bolometric luminosity had decreased by a factor of five over three months! Note also the discrepant H/He abundance pattern resulting from analysis of the two datasets in Table 6.

The mass-loss rate for HD 5980 during its brief eruption compares very closely with V1. It appears that ‘giant eruptions’ of LBV’s in low metallicity environments exhibit representative mass-loss rates approaching  $\sim 10^{-3} M_\odot \text{yr}^{-1}$ . These differ greatly from the sole source of mass-loss rate produced in giant LBV eruptions known to date, namely the famous Homunculus produced by  $\eta$  Car between 1837–1960. During this eruption,  $\sim 2 - 3 M_\odot$  were ejected (Davidson & Humphreys 1997) corresponding to  $\sim 10^{-1} M_\odot \text{yr}^{-1}$ . Thus far,  $\eta$  Car appears to be unique in exhibiting such high rates of mass-loss, namely during its 1840’s eruption. Indeed, although not presently in outburst,  $\eta$  Car remains a very extreme star, as illustrated in Figure 10, with a present luminosity and mass-loss rate somewhat higher than V1 (see also Table 6). Hence, the present V1 outburst should not be considered an equivalent to the great  $\eta$  Car 1837–1860 eruption.

## 5. CONCLUSIONS

From our quantitative analysis of an HST/STIS spectrogram of NGC 2363-V1, and a photometric follow-up of this star since the beginning of its present eruption, we conclude as follows. V1 is a Luminous Blue Variable currently experiencing a major eruption. Its immediate progenitor star was probably an initial  $\approx 60 M_\odot$  late O supergiant.

Its physical parameters are exceptional:  $\log(L/L_\odot) = 6.35$ ,  $T_* = 11\text{kK}$ ,  $R_* = 420 R_\odot$  for 1997 November; and  $\log(L/L_\odot) = 6.4$ ,  $T_* = 13\text{kK}$ ,  $R_* = 315 R_\odot$  for 1999 July. Therefore, the bolometric luminosity of V1 is exceeded by only, in ascending order,  $\eta$  Car ( $\log L/L_\odot = 6.7$ , Hillier et al. 2000), the Pistol star ( $\log L/L_\odot = 6.9 \pm 0.3$ , Figer et al. 1998) and HD 5980 during eruption ( $\log L/L_\odot = 7.1$ ).

Analysis of high resolution  $\text{H}\alpha$  observations indicate that the wind is moderately clumped, with  $\dot{M} \simeq 4.5 \times 10^{-4} M_\odot \text{ yr}^{-1}$  and  $v_\infty \simeq 300 \text{ km s}^{-1}$ . During its brief eruption in 1994, HD 5980 possessed a similar mass-loss rate. Therefore, the mass-loss rate of  $\sim 10^{-1} M_\odot \text{ yr}^{-1}$  exhibited by  $\eta$  Car during its giant eruption in 1840’s (Humphreys & Davidson 1994) is thus far unique.

The presence of many iron features in the spectrum permits an estimate of its heavy metal content.

Although discrepancies remain, especially at UV wavelengths, our study reveals a SMC-like Fe content for NGC 2363-V1, which is in good agreement with previously derived oxygen abundances for NGC 2363. Consequently, the heavy metal enrichment of NGC 2363, produced by Type I Supernovae, whose progenitors are believed to have a lifetime of typically 1 Gyr, appears to mimic that of light elements, such as oxygen, which are created exclusively by short-lived (10 Myr) massive stars.

Observationally, spectroscopic and photometric monitoring of V1 and other LBVs will continue, while theoretical studies are underway to investigate the cause of the outbursts experienced by V1 and HD 5980, whether pulsationally, dynamically or rotationally driven.

We would like to thank Mohammad Heydari-Malayeri for providing the outburst spectrum of HD 5980, Albert Jones for providing his photometry of HD 5980, and Kris Davidson and his HST/STIS observing team for providing the spectrum of Eta Carina in Figure 10. This investigation was funded in part by the Natural Sciences and Engineering Research Council of Canada, by the Fonds FCAR of the Government of Québec and by Université Laval (LD, JRR and CR). PAC acknowledges financial support from the Royal Society. We are especially grateful to the staff of the now defunct Royal Greenwich Observatory for obtaining service imaging of NGC 2363. The William Herschel Telescope is operated on the Island of La Palma by the Isaac Newton Group in the Spanish Observatorio del Roque de los Muchachos of the Instituto de Astrofísica de Canarias.

## REFERENCES

Anderson, L. S. 1989, *ApJ*, 339, 558

Barba, R., & Niemela, V. S. 1994, *IAU Circ.* 6099

Bouchet, P., Lequeux, J., Maurice, E., Prevot, L., & Prevot-Burnichon, M. L. 1985, *A&A*, 149, 330

Crowther, P. A. 1997, in: *ASP Conf. Ser.* 120, *Luminous Blue Variables, Massive Stars in Transition*, eds. Nota, A. & Lamers, H. J. G. L. M., 51

Crowther, P. A., 2000, *A&A*, 356, 191

Davidson, K., Dufour, R. J., Walborn, N. R., & Gull, T. R. 1986, *ApJ*, 305, 867

Davidson, K. & Humphreys, R. M. 1997, *ARA&A*, 35, 1

Drissen, L., Roy, J.-R., & Robert, C. 1996, *IAU Circ.* 6294

Drissen, L., Roy, J.-R., & Robert, C. 1997, *ApJ*, 474, L35 (DRR97)

Drissen, L., Roy, J.-R., Robert, C., Devost, D., & Doyon, R. 2000, *AJ*, 119, 688

Eversberg, T., Lépine S., & Moffat, A. F. J. 1998, *ApJ*, 494, 799

Figer, D. F., Najarro, F., Morris, M., McLean, I. S., Geballe, T. R., Ghez, A. M., & Langer, N. 1998, *ApJ*, 506, 384

Guzik, J. A., Cox, A. N., Despain, K. M. 1999, in: *ASP Conf. Ser.* 179, *Eta Carina at the Millennium*, eds. Morse, J. A., Humphreys, R. M., & Daminelli, A., 347

Gonzalez-Delgado, R. M., Perez, E., Tenorio-Tagle, G., Vilchez, J. M., Terlevich, E., et al. 1994, *ApJ*, 437, 239

Herrero, B., Cooper, L. L., Dickinson, A. S., & Flower, D. R. 1995, *J. Phys. B.*, 28, 711

Heydari-Malayeri, M., Rauw, G., Esslinger, O., & Beuzit, J.-L. 1997, *A&A*, 322, 554

Hillier, D. J. 1991, *A&A*, 247, 455

Hillier, D. J., & Miller, D. 1998, *ApJ*, 496, 407

Hillier, D. J., Crowther, P. A., Najarro, F., & Fullerton, A. W. A. 1998, *A&A*, 340, 483

Hillier, D. J., Davidson, K., Ishibashi, K., & Gull, T. 2000, *ApJ*, submitted

Holtzman, J. A., et al. 1995, *PASP*, 107, 156

Hummer, D. G., & Storey, P. J. 1995, *MNRAS*, 272, 41

Humphreys, R. M., & Davidson, K. 1994, *PASP*, 106, 1025

Kaiser, D. 1987, *A&AS*, 67, 203

Koenigsberger, G., Pena, M., Schmutz, W., & Ayala, S. 1998, *ApJ*, 499, 889

Kurucz, R. L. 1993, *CD-ROM 23* (Cambridge: Smithsonian Astrophysical Observatory)

Landolt, A. U. 1992, *AJ*, 104, 340

Leitherer, C., Allen, R., Altner, B., et al. 1994, *ApJ*, 428, 292

Lépine, S., & Moffat, A. F. J. 1999, *ApJ*, 514, 909

Luridiana, V., Peimbert, M., & Leitherer, C. 1999, *ApJ*, 527, 110

Massa, D. 1989, *A&A*, 224, 131

Meynet, G., Maeder, A., Schaller, G., Schaerer, D., & Charbonnel, C. 1994, *A&AS*, 103, 97

Nahar, S. N. 1995, *A&A*, 392, 967

Nemry, F., Surdej, J., & Hernaiz, A. 1991, *A&A*, 247, 469

Neufeld, D. A., & Dalgarno, A. 1987, *Phys. Rev. A*, 35, 3142

Nota, A., & Lamers, H. J. G. L. M. (eds.) 1997, *ASP Conf. Ser. 120, Luminous Blue Variables: Massive Stars in Transition*

Nota, A., Livio, M., Clampin, M., & Schulte-Ladbeck, R. 1995, *ApJ*, 448, 788

Prinja, R. K. 1990, *MNRAS*, 246, 392

Puls J., et al. 1996, *A&A*, 305, 171

Robert, C. 1999, in: *ASP Conf. Ser. 192, Spectrophotometric Dating of Stars and Galaxies*, eds. Hubeny, I, Heap, S. R., & Cornett, R.-H., 16

Seaton, M. J. 1979, *MNRAS*, 187, 73

Smith, L. J., Crowther, P. A., & Prinja, R. K. 1994, *A&A*, 281, 833

Snow, T. P., & Morton, D. C. 1976, *ApJS*, 32, 429

Stahl, O., Wolf, B., Klare, G., Jüttner, A., & Cassatella, A. 1990, *A&A*, 228, 379

Stetson, P. B. 1987, *PASP*, 99, 191

Stothers, R. B. 1999a, *ApJ*, 513, 460

Stothers, R. B. 1999b, *ApJ*, 516, 366

Tolstoy, E., Saha, A., Hoessel, J. G., & McQuade, K. 1995, *AJ*, 110, 1640

Vacca, W. D., Garmany C. D., & Shull J. M. 1996, *ApJ*, 460, 914

Walborn, N. R., Parker, J. Wm., & Nichols, J. S. 1995, *IUE Atlas of B-type spectra from 1200 to 1900 Å*, NASA Ref. Pub. 1363

Walborn, N. R., Drissen, L., Parker, J. Wm., Saha, A., MacKenty, J.W., & White, R. L. 1999, *AJ*, 118, 1684

Westerlund, B. E. 1997, *The Magellanic Clouds* (Cambridge)

Whitmore, B. 1995, Proc. Calibrating Hubble Space Telescope, eds Koratkar, A., & Leitherer, C. (STScI: Baltimore), 269

Table 1. Photometric variability of NGC 2363-V1 since 1996

Epoch	Observatory	F170W	U	B	V	R	F1042M
1996 Jan	HST/WFPC2	—	—	17.82	17.88	—	—
1997 Nov	HST/STIS	17.25	16.79	17.55	17.43	17.16	—
1998 Jan	WHT/aux	—	16.13	17.53	17.66	17.33	—
1998 Mar	HST/WFPC2	17.23	16.72	—	17.52	—	17.15
1998 Dec	HST/WFPC2	17.09	16.79	—	17.55	—	17.20
1999 Jul	HST/STIS	16.83	16.85	17.72	17.58	17.20	—
1999 Nov	HST/WFPC2	16.89	16.89	—	17.80	—	17.56
2000 Feb	HST/WFPC2	16.98	16.72	—	17.76	—	17.50

Table 2. Equivalent widths of the Balmer lines in V1

Line	$W_\lambda$ (1997)	$W_\lambda$ (1999)
H $\alpha$	250	300
H $\beta$	45	35
H $\gamma$	15	11
H $\delta$	6	5

Note. — The equivalent width, in units of Å, is for the emission component only.

Table 3. Equivalent widths of the the strongest UV lines in V1 and NGC 2363

Line	$W_\lambda$ (V1) (Å)	$W_\lambda$ (knot A) (Å)	$W_\lambda$ (knot B) (Å)
C III $\lambda$ 1175	2.4	—	—
Si II $\lambda$ 1260	2.8	0.9	1.6
Si II $\lambda$ 1265	1.8	—	—
O I/Si II $\lambda$ 1303	4.1	2.2	2.3
Si II $\lambda$ 1309	1.0	—	—
C II $\lambda$ 1334	2.5	1.6	1.6
Si IV $\lambda$ 1393	2.0	0.6	0.6
Si IV $\lambda$ 1402	2.3	0.5	1.1
Si II $\lambda$ 1527	2.1	0.8	0.8
Si II $\lambda$ 1533	1.9	$\leq$ 0.2	$\leq$ 0.1
C IV $\lambda$ 1549,51	2.8	—	2.1

Table 4. Summary of model atoms used in radiative transfer calculations

Ion	$N_S$	$N_F$	$N_{\text{Trans}}$	Details
H I	10	30	435	$n \leq 30$ .
He I	27	39	315	$n \leq 14$
He II	5	5	10	$n \leq 5$
N I	44	104	855	$nl \leq 5f2F^\circ$
N II	23	41	144	$nl \leq 2p3d1P^\circ$
N III	8	8	11	$nl \leq 2p3^2P^\circ$
Na I	18	53	507	$n \leq 12$
Mg II	18	45	362	$n \leq 10$
Al II	26	44	171	$nl \leq 5d1D$
Al III	12	20	67	$n \leq 5$
Ca II	17	58	463	$n \leq 11$
Si II	31	49	281	$nl \leq 3s^29h2H^\circ$
Si III	12	20	42	$nl \leq 3s4p1P^\circ$
Fe II	134	827	21907	$nl \leq 3d^5(^6S)4p^2(^3P)^4P$
Fe III	69	607	6620	$nl \leq 3d^5(^4D)6s^3D$

Note. — Including full levels ( $N_F$ ), super levels ( $N_S$ ) and total number of transitions ( $N_{\text{Trans}}$ ), following Hillier & Miller (1998).

Table 5. Estimates of stellar properties for NGC 2363-V1 prior to outburst

Sp. Type	$T_{\text{eff}}$ kK	$R_*$ $R_{\odot}$	$\log L_*$ $L_{\odot}$	$\log \dot{M}$ $M_{\odot} \text{yr}^{-1}$	$v_{\infty}$ $\text{km s}^{-1}$
O3 I	50.7	18	$\leq 6.27$	-5.3	3200
O8 I	35.7	22	$\leq 5.85$	-6.2	2000
B0.5 I	25.6	27	$\leq 5.46$	-5.8	250

Note. — We use here the temperature and bolometric correction scale from Vacca et al. (1996), plus the wind momentum–luminosity relation of Puls et al. (1996) for low metallicity (LMC and SMC) OB stars, except for the early B supergiant for which typical LBV wind properties are shown (Crowther 1997).

Table 6. Stellar parameters of V1 and of other well known LBVs

Star	Epoch	$T/\text{kK}$ $\tau_{\text{Ross}}=10$	$R/R_{\odot}$ $\tau_{\text{Ross}}=2/3$	$\log L_*$ $L_{\odot}$	$\log \dot{M}/\sqrt{f}$ $M_{\odot} \text{yr}^{-1}$	$v_{\infty}$ $\text{km s}^{-1}$	H/He	$M_V$ mag	Reference
NGC 2363-V1	Nov 1997	11	590	6.35	-3.1	325	4.0?	-10.4	This work
	Jul 1999	13	675	6.4	-3.1	290	4.0?	-10.3	This work
HD 5980	Sep 1994	23	280	7.05	-3.1	500	0.7	-10.5	This work
	Dec 1994	35	130:	6.5	-3.0	600	2.5	-8.6	(1)
$\eta$ Car	Mar 1998	27	881	6.7	-2.5	500	5?	-?	(2)

Note. — We estimate that a volume filling factor of  $f=0.3$  is appropriate for V1, with  $f=0.1$  for  $\eta$  Car and HD 5980. References: (1) Koenigsberger et al. (1998); (2) Hillier et al. (2000).

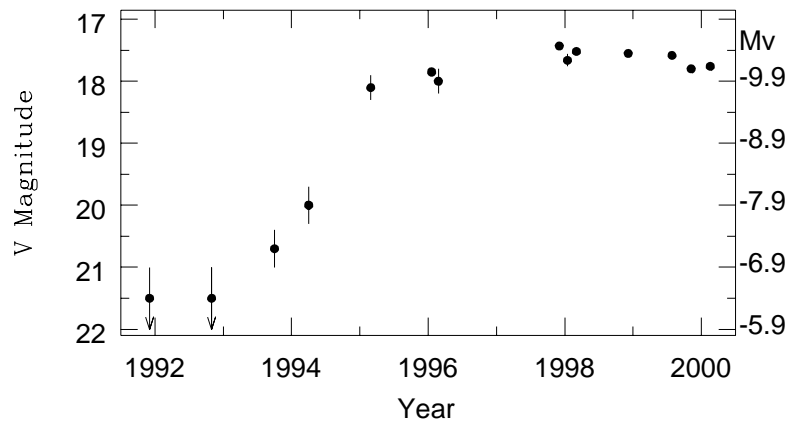


Fig. 1.— V-band light curve of NGC 2363-V1 over the past 7 years. The absolute magnitude scale on the right assumes a distance of 3.44 Mpc and  $E(B - V) = 0.06$  (see text).

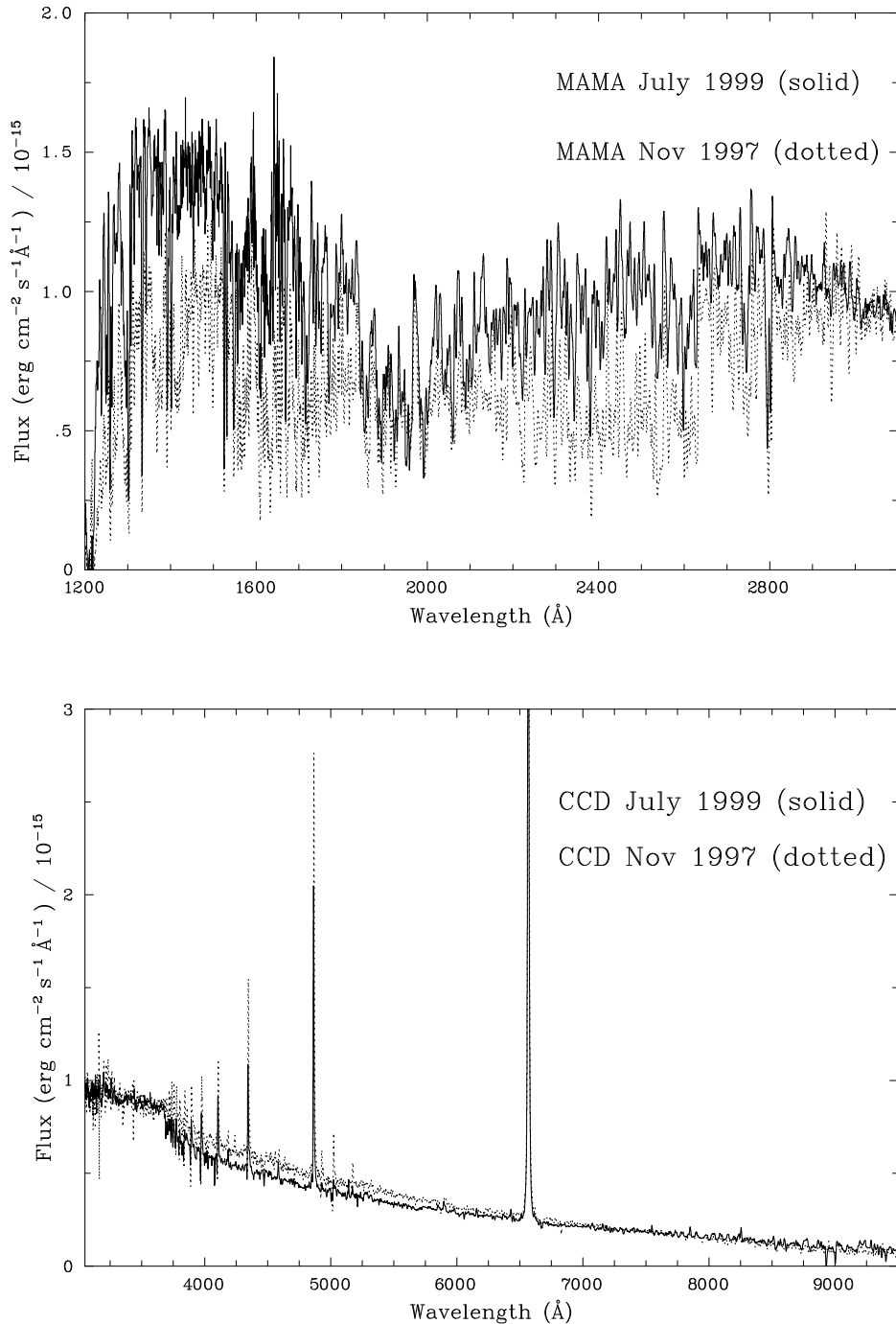


Fig. 2.— Flux calibrated HST/STIS spectrogram of V1 from 1999 July (solid) and 1997 November (dotted). The ripples longward of 7500 Å are due to fringing on the CCD.

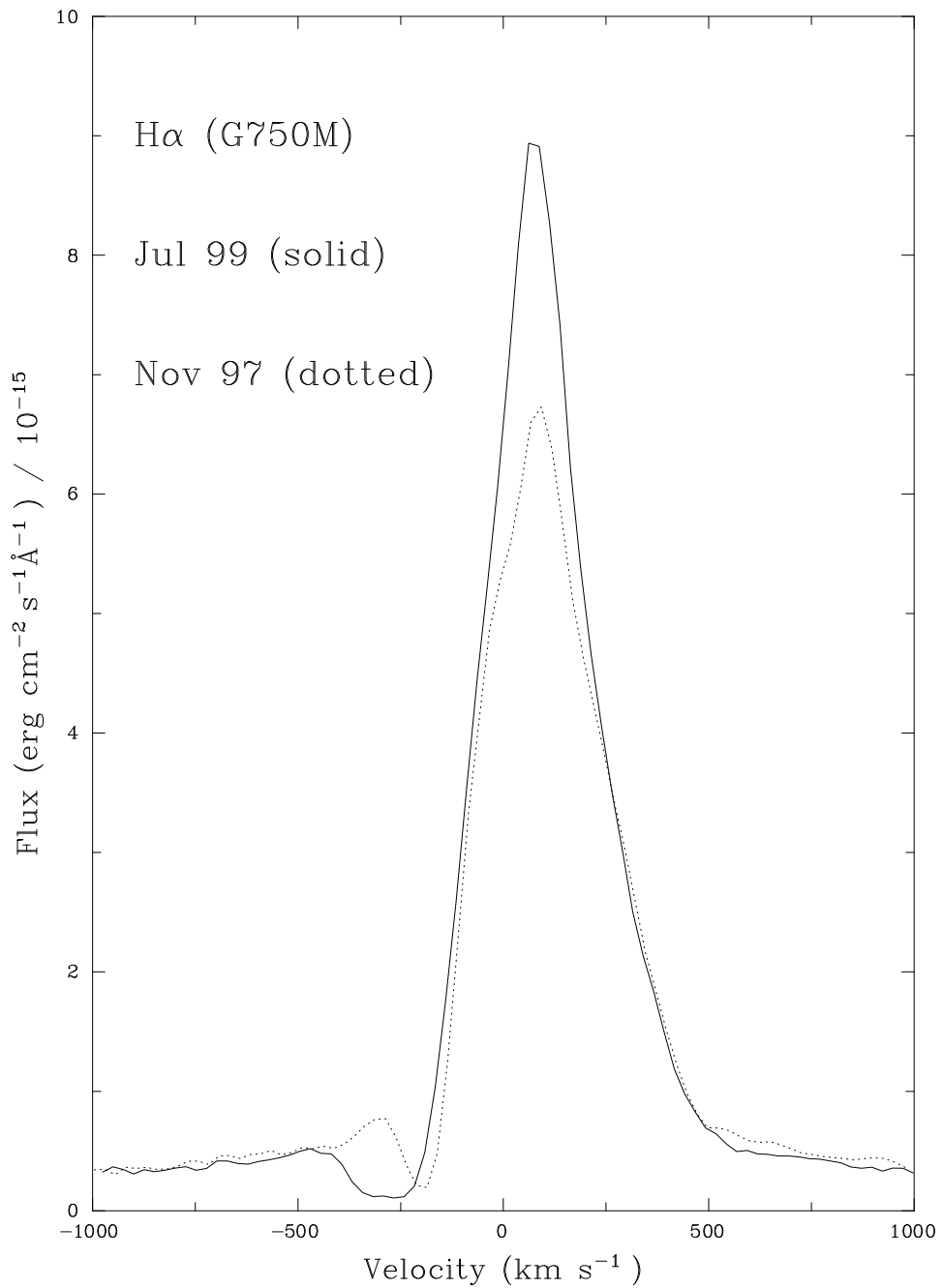


Fig. 3.— High resolution HST/STIS spectrogram of V1 (grating G750M), revealing a P Cygni H $\alpha$  profile.

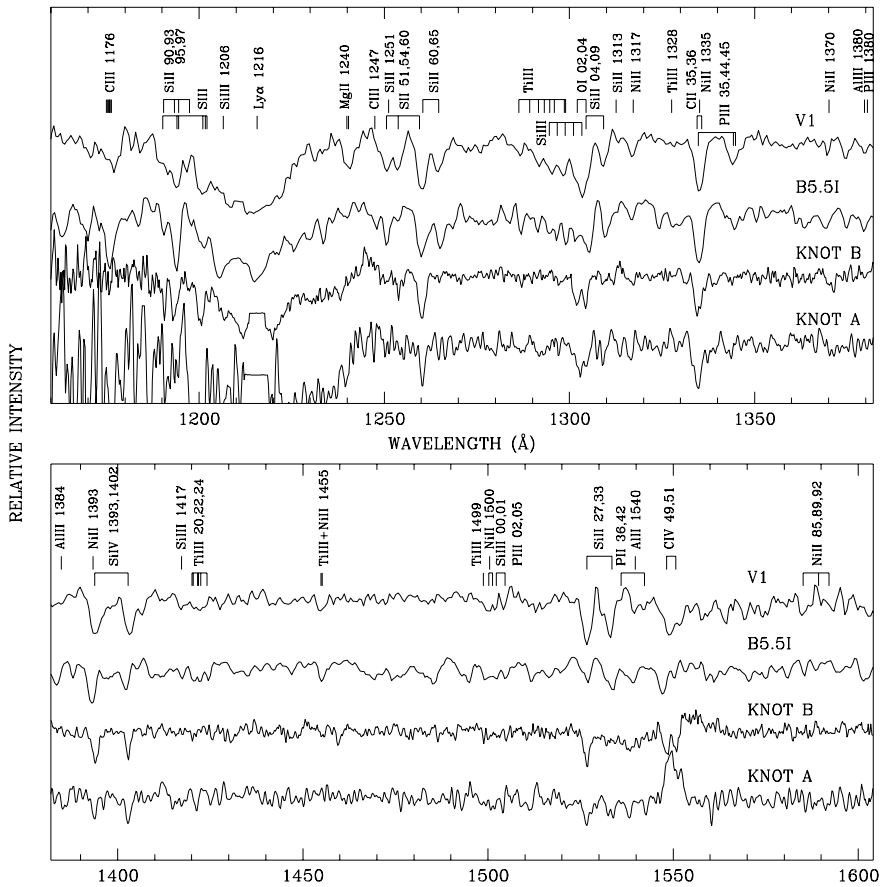


Fig. 4.— Rectified spectra of NGC 2363-V1 in 1999, NGC 2363-A, NGC 2363-B and a representative Galactic B5.5I spectrum (see text).

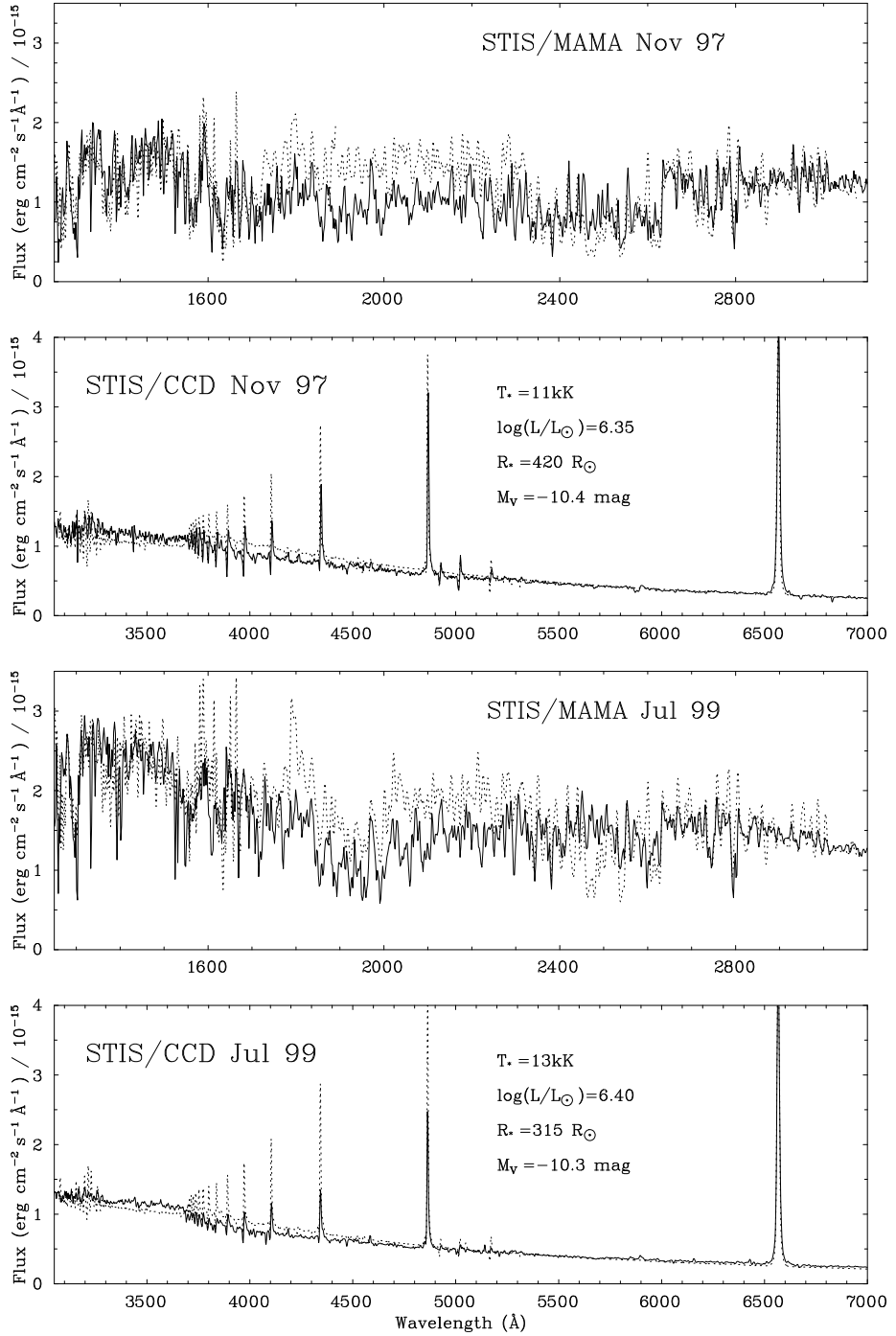


Fig. 5.— Comparison between de-reddened HST/STIS datasets (solid) from 1997 November (upper panels) or 1999 July (lower panels) with non-LTE model predictions (dotted).

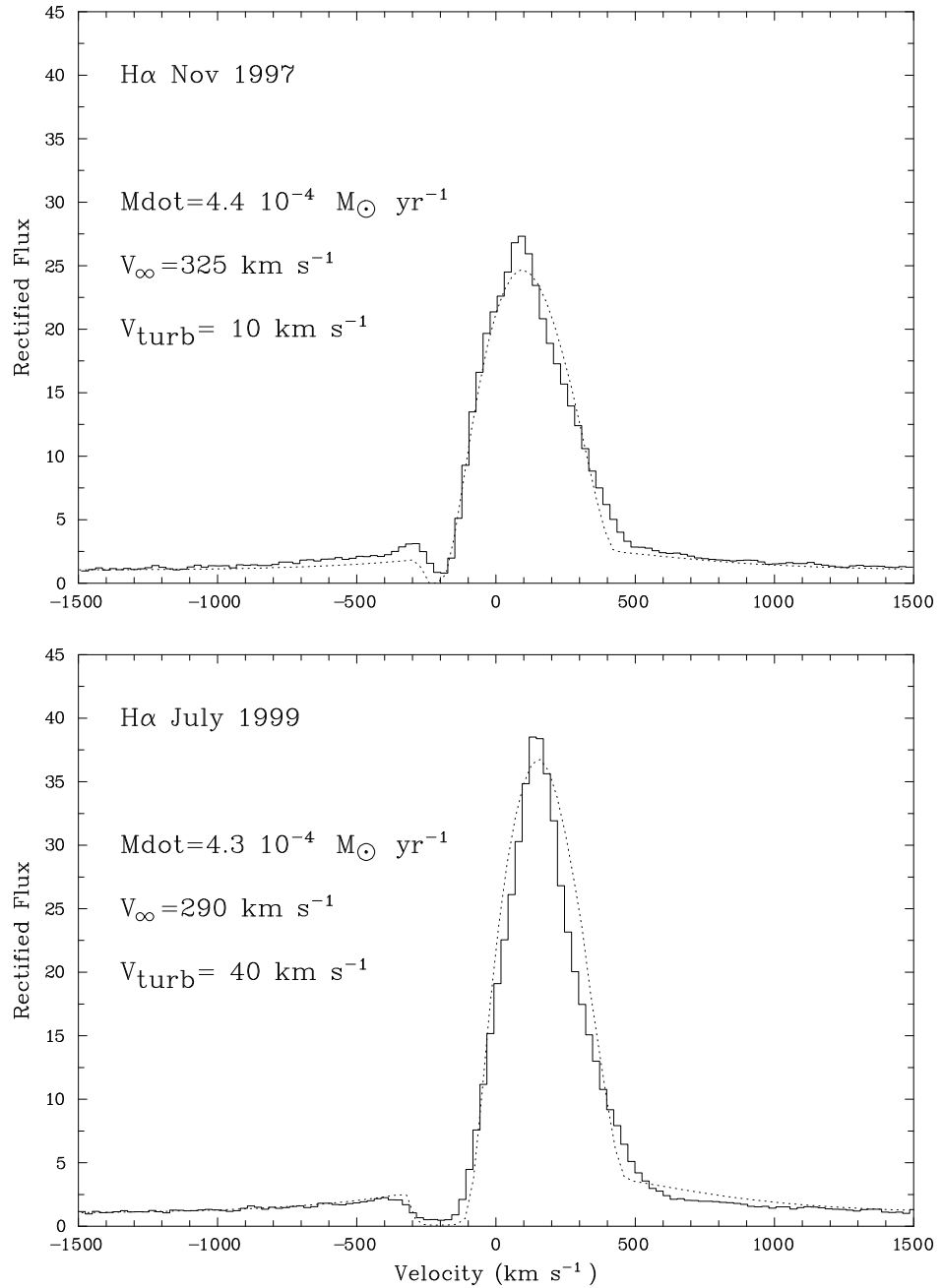


Fig. 6.— Comparison between rectified H $\alpha$  profiles (solid) and synthetic spectra (dotted).

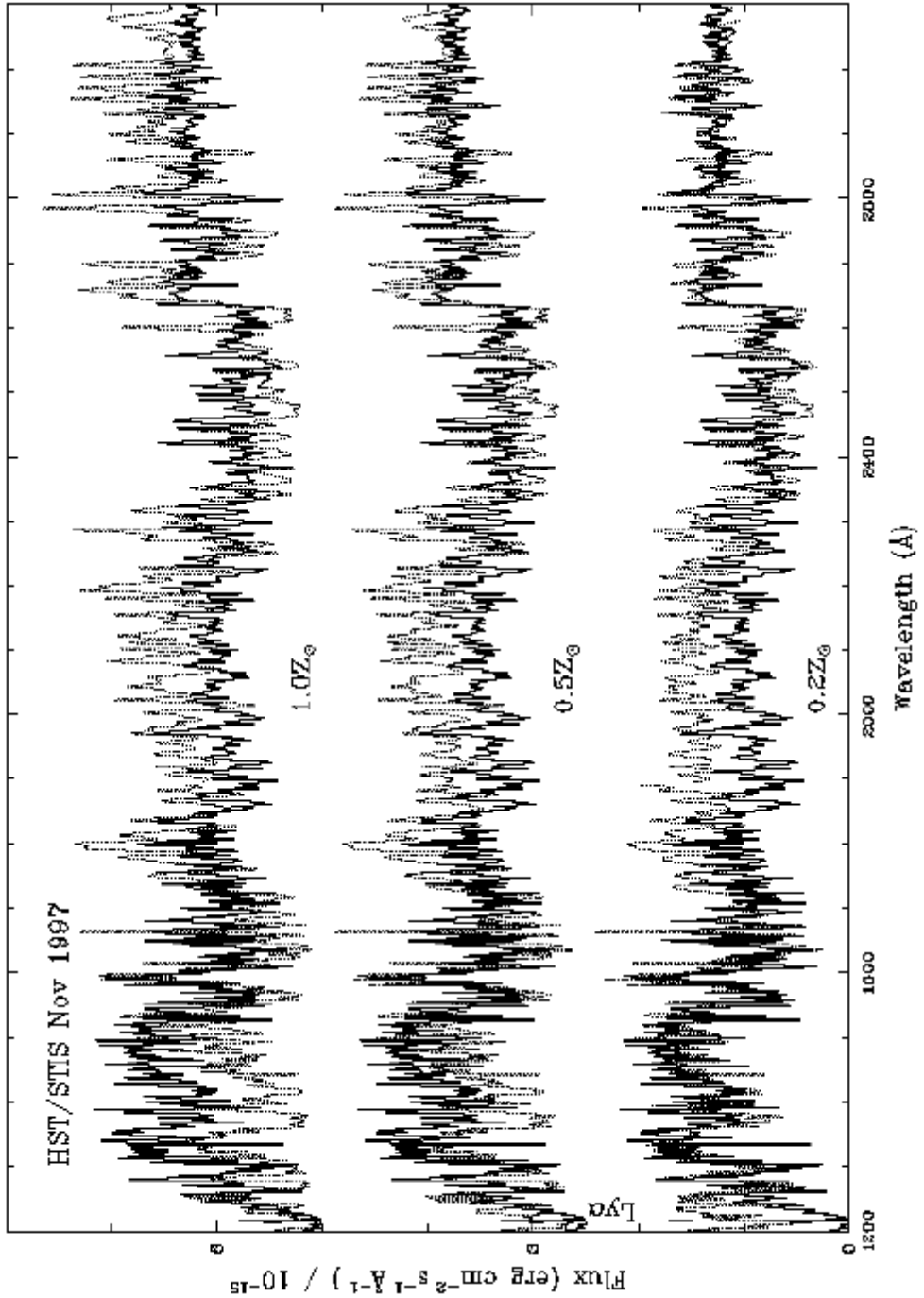


Fig. 7.— Comparison between de-reddened STIS/MAMA datasets of V1 with line blanketed UV energy distributions, for  $0.20Z_{\odot}$  (lower),  $0.5Z_{\odot}$  (middle),  $1.0Z_{\odot}$  (upper), for clarity successively offset by  $2.5 \times 10^{-15}$   $\text{erg cm}^{-2} \text{s}^{-1} \text{\AA}$ .

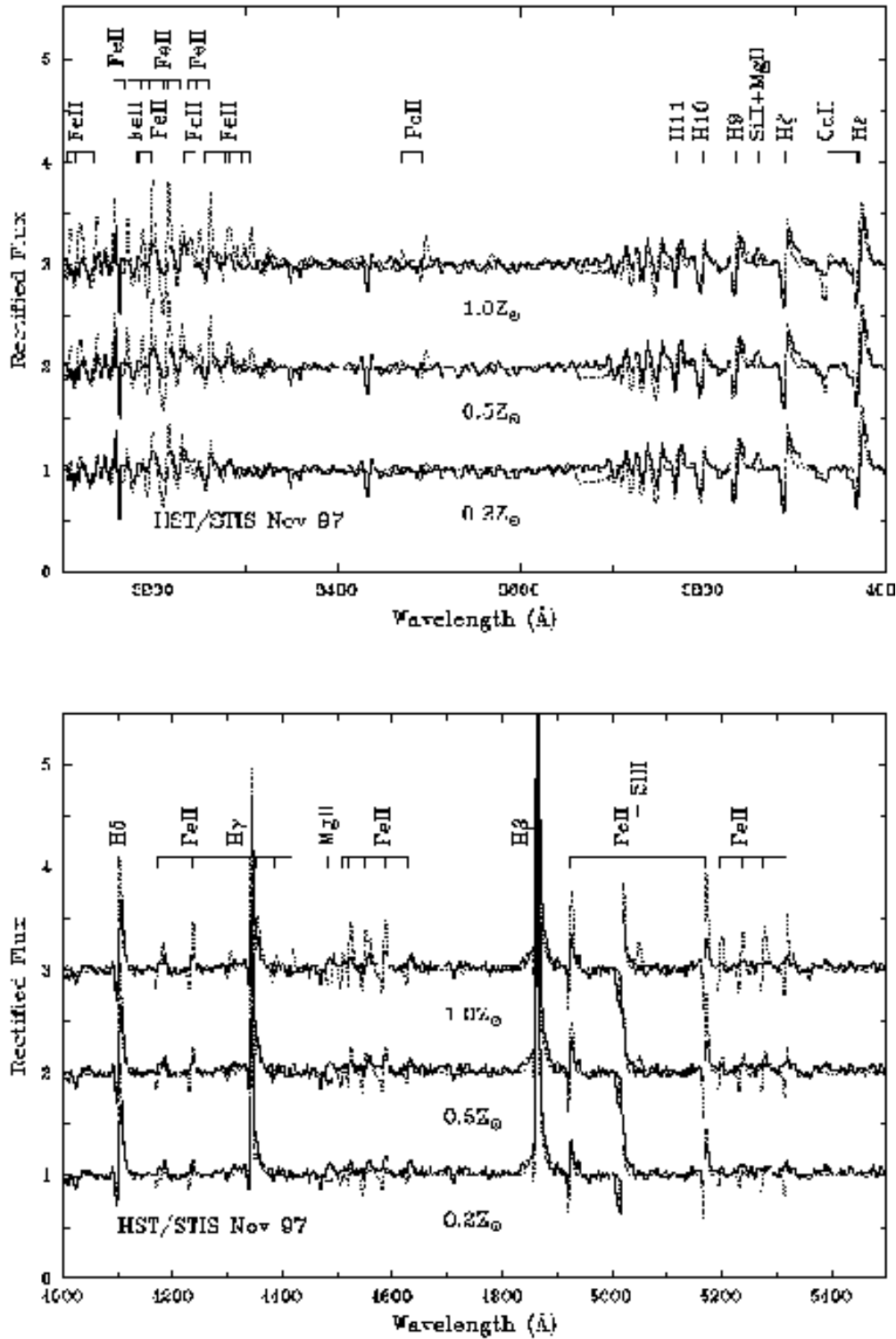


Fig. 8.— Comparison between rectified, optical STIS datasets of V1 with line blanketed energy distributions, for  $0.20Z_{\odot}$  (lower),  $0.5Z_{\odot}$  (middle),  $1.0Z_{\odot}$  (upper), for clarity successively offset by a continuum unit.

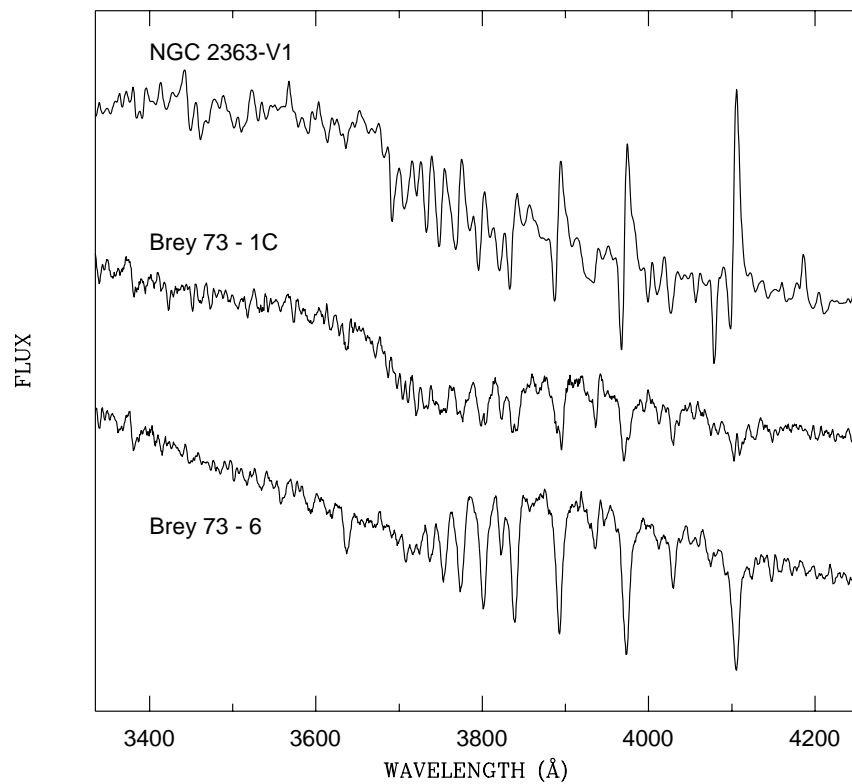


Fig. 9.— Comparison between V1 and two LMC B stars in the Breysacher 73 cluster, # 1C (O9.5-B1pe) and # 6 (B0.2V), in the vicinity of the Balmer jump.

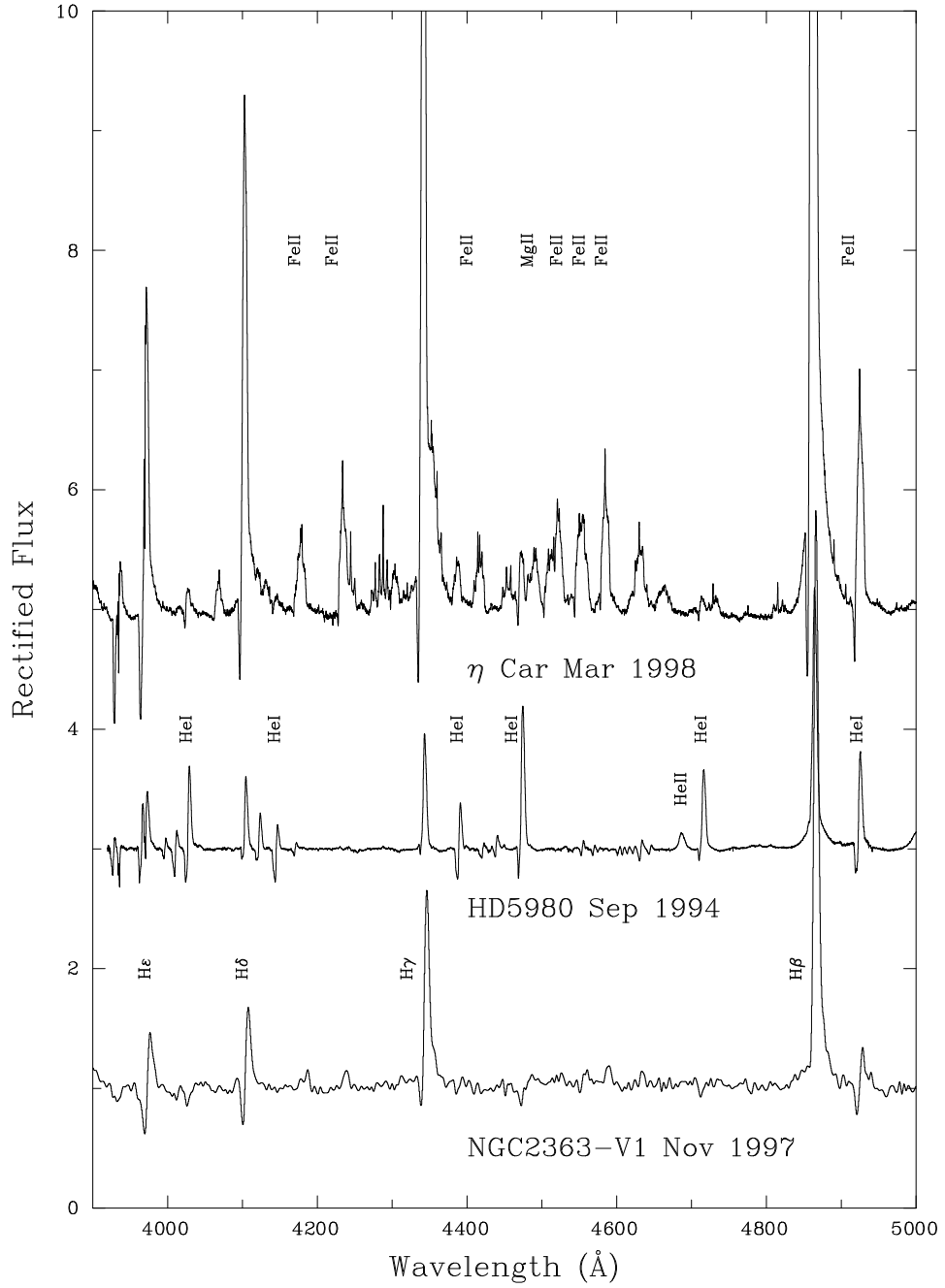


Fig. 10.— Comparison between rectified, optical datasets of V1 with HD 5980 during outburst in 1994 September, plus  $\eta$  Car in 1998 March (HST/STIS data from Davidson *et al.*, in preparation).